



# Combined effects of polymer SH and ryegrass on the water-holding characteristics of loess

YING Chunye<sup>1</sup>, LI Chenglong<sup>2</sup>, LI Lanxing<sup>3\*</sup>, ZHOU Chang<sup>4</sup>

<sup>1</sup> School of Geological Engineering, Qinghai University, Xining 810016, China;

<sup>2</sup> Petroleum Engineering Technology Research Institute of Shengli Oilfield, SINOPEC, Dongying 257000, China;

<sup>3</sup> Army Engineering University of PLA, Xuzhou 221000, China;

<sup>4</sup> School of Resources and Geosciences, China University of Mining and Technology, Xuzhou 221116, China

**Abstract:** The Chinese Loess Plateau has long been plagued by severe soil erosion and water scarcity. In this study, we proposed a technique involving the combined use of polymer SH and ryegrass and evaluated its effectiveness in modifying the water-holding characteristics of loess on the Chinese Loess Plateau (Chinese loess). We analysed the volumetric water content and water potential of untreated loess, treated loess with single polymer SH, treated loess with single ryegrass, and treated loess with both polymer SH and ryegrass using the loess samples collected from the Chinese Loess Plateau in July 2023. Moreover, fractal theory was used to analyse the fractal characteristics of the soil structure, and wet disintegration tests were conducted to assess the structural stability of both untreated and treated loess samples. The results showed that the loess samples treated with both polymer SH and ryegrass presented much higher volumetric water content and water potential than the untreated loess samples and those treated only with ryegrass or polymer SH. Moreover, the planting density of ryegrass affected the combined technique, since a relatively low planting density (20 g/m<sup>2</sup>) was conducive to enhancing the water-holding capacity of Chinese loess. The fractal dimension was directly correlated with both volumetric water content and water potential of Chinese loess. Specifically, since loess treated with both polymer SH and ryegrass was more saturated with moisture, its water potential increased, thus improving its water-holding capacity and fractal dimension. The combined technique better resisted disintegration than ryegrass alone but had slightly less resistance than polymer SH alone. This study provides insight into soil reinforcement and soil water management using polymetric materials and vegetation on the Chinese Loess Plateau.

**Keywords:** loess; ryegrass; polymer SH; water-holding characteristics; fractal theory; Chinese Loess Plateau

**Citation:** YING Chunye, LI Chenglong, LI Lanxing, ZHOU Chang. 2024. Combined effects of polymer SH and ryegrass on the water-holding characteristics of loess. *Journal of Arid Land*, 16(12): 1686–1700. <https://doi.org/10.1007/s40333-024-0089-9>; <https://cstr.cn/32276.14.JAL.02400899>

## 1 Introduction

The Chinese Loess Plateau, which is one of the most well-known areas, is the largest loess deposit in the world in terms of both depth and area (Huang and Shao, 2019). It is characterized by severe soil erosion and water scarcity. The soil water-holding characteristics refer to the soil's ability to retain water and describe the relationship between soil suction and humidity (degree of saturation, gravity water content, or volumetric water content). These characteristics are closely related to the deformation, strength, and permeability of unsaturated soil (Vanapalli et al., 1996;

\*Corresponding author: LI Lanxing (E-mail: lilanxing0531@cug.edu.cn)

Received 2024-07-29; revised 2024-10-30; accepted 2024-11-01

© Xinjiang Institute of Ecology and Geography, Chinese Academy of Sciences, Science Press and Springer-Verlag GmbH Germany, part of Springer Nature 2024

Fredlund, 2006). The water-holding characteristics of loess on the Chinese Loess Plateau (Chinese loess) have significant direct impacts on food security, human health, and the overall functioning of ecosystems (Gomiero, 2016; Chen et al., 2024). Current efforts concentrate on modifying the water-holding characteristics of Chinese loess by implementing various measures such as vegetation cover (Zhang et al., 2021c; Qiu et al., 2024), chemical materials (Zhang et al., 2021b; Zhang et al., 2023), and biogeochemical improvements (Xue et al., 2022; Yang et al., 2022).

Among chemical materials, the polymer SH, which is an organic polymer curing material that originates from Lanzhou University, China (Chen et al., 2017), has numerous advantages. These advantages include low viscosity, non-toxic composition, cost efficiency, ease of application, adjustable gelation time, complete solubility in water, and exceptional homogeneity when blended with soil (Wang et al., 2005). As a result, it has broad application prospects in the modification of ecology. Currently, its application has been extended from the initial loess improvement to granite residual soil (Yuan et al., 2023) and coarse-grained soil at earthen ruins (Zhang et al., 2020). Extensive studies have demonstrated that the polymer SH treatment significantly improves various soil properties of loess, including liquid limit, plastic limit, unconfined compression strength, tensile strength, shear strength, water stability, low-temperature resistance, and ability to withstand dry-wet cycles and freeze-thaw cycles (Qin et al., 2008; Chen et al., 2017; Zhang et al., 2021a). Moreover, a notable decrease in accumulative sediment yield and collapsibility of polymer SH-treated soil was observed (Ying et al., 2024). Due to the positive effects of polymer SH on loess, polymer SH can protect the loess slope by forming protective layers that maintain the good water-holding capacity of loess and increase the erosion resistance of loess (Li et al., 2016).

Vegetation is an important measure to modify soil water-holding characteristics (Shi and Shao, 2000; Haruna et al., 2020). In general, plants contribute to increasing the water-holding capacity of soil through various mechanisms, including water absorption by their roots (Leenaars et al., 2018), shading to reduce evaporation (Williams et al., 1993), increasing soil cohesion (Suzuki et al., 2007), providing plant litter coverage (Xie and Su, 2020), improving the soil structure (Suzuki et al., 2007), enhancing microbial activities (Zheng et al., 2018), and increasing the organic matter content (Lal, 2020). These functions are interrelated and interdependent, and collectively sustain the stability and sustainability of the soil ecosystem. As a typical vegetation for soil and water conservation, ryegrass has been successfully used in America (Malik et al., 2000), Brazil (Ramos et al., 2014), Portugal (Trindade et al., 2009), and China (Zhou and Shangguan, 2008), among other countries. Ryegrass can increase the organic matter content of loess, adjust the soil temperature, decrease the wind speed and relative light intensity, and improve the water-holding capacity of loess (Li et al., 2009). Additionally, ryegrass planting can effectively control soil erosion and reduce soil sediment yield and runoff (Zhou and Shangguan, 2007; Zhou and Shangguan, 2008; Dong et al., 2015); thus, it affects soil water-holding characteristics. The ability of ryegrass to enhance soil water-holding characteristics is directly associated with the changes in soil physicochemical properties during the growth process of ryegrass. Specifically, when ryegrass grows, its root activities and the decomposition of organic matter modify the soil structure, increase soil porosity, and consequently enhance soil water-holding capacity (Angers and Caron, 1998; Koudahe et al., 2022). An experiment on ryegrass with growth periods of 4–16 weeks revealed that with the prolonged growth of ryegrass in loess, soil bulk density gradually decreased, whereas water stable aggregates and organic matter contents progressively increased (Qin, 2016). However, the growth of herbaceous vegetation is a long-term process, and long-term monitoring is necessary to accurately reflect the impact of vegetation on soil properties.

Polymer SH or ryegrass alone can effectively modify the water-holding characteristics of loess. Ryegrass can penetrate deeply into the loess with its well-developed root system. This penetration stabilizes the loess particles to reduce soil erosion, absorbs water from the ground through

transpiration, and consequently increases the water-holding capacity of loess (Ying et al., 2024). Meanwhile, polymer SH can form stable aggregate structures in loess due to its unique three-dimensional network structure, which enhances the porosity, permeability and water-holding capacity of loess (Qin et al., 2008; Zhang et al., 2021a). During its degradation process, polymer SH can provide nutrients for ryegrass and promote its growth (Ying et al., 2024). However, current research into the combined effects of polymer SH and ryegrass on the water-holding characteristics of loess remains inadequate.

Understanding the intricate relationship between soil structure and its water-holding capacity is crucial, necessitating the exploration of advanced methods to accurately model and interpret these dynamics. To facilitate this, experimental data obtained from the soil-water characteristic curve test, which tend to be discrete, are typically fitted using mathematical models. Commonly used models are Campbell model (Jabro et al., 2009; Pittaki-Chrysodonta et al., 2018) and van Genuchten model (Ghanbarian-Alavijeh et al., 2010; Wei et al., 2019). However, the physical meanings of the parameters in these models are often unclear, and accurately determining these parameters can be challenging. In contrast, the fractal method, which uses fractal theory to determine the soil-water characteristic curve, provides parameters that are directly related to the properties of the soil structure and have clear physical meanings (Comegna et al., 1998; Yang et al., 2023). This renders the fractal method an ideal approach to fit the soil-water characteristic curve and provide insights into the soil structure and its relationship with water-holding capacity.

The primary objectives of this study are to: (1) evaluate the combined effects of polymer SH and ryegrass on the water-holding characteristics of Chinese loess; and (2) investigate the relationship between soil structure and water-holding capacity using fractal theory. To achieve these objectives, we designed an experiment including six groups of loess samples, and monitored the volumetric water content and water potential of loess samples during the growth of ryegrass to quantify changes in water-holding capacity. Furthermore, fractal theory was applied to analyse the soil structure and offer deeper insights into the underlying mechanisms of the observed changes. The outcomes of this study are anticipated to clarify the synergistic effects of polymeric materials and vegetation, and help formulate efficient soil stabilization and water management strategies for the Chinese Loess Plateau.

## 2 Materials and methods

### 2.1 Materials

#### 2.1.1 Loess

The loess in this study was collected in July 2023 from a gentle slope in Zichang County, Shaanxi Province, which is located on the Chinese Loess Plateau (Fig. 1). The sampling depth of the tested loess was 20.0 cm below the surface of the gentle slope. According to Zeng and Huang (2010), the loess examined from this region exhibited a meta-stable structure characterized by high porosity, low bearing pressure on the foundation, and remarkable collapsibility.

The particle size distribution of loess samples was determined through sieve analysis and hydrometer testing. The grading criteria for the soil particle size were based on the Standard for Engineering Classification of Soil (Ministry of Housing and Urban-Rural Development of the People's Republic of China, 2008), according to which the samples comprised 11.09% clay (particle size ( $d \leq 0.005$  mm), 87.39% silt ( $0.005 \text{ mm} < d \leq 0.075$  mm), and 1.52% sand ( $0.075 \text{ mm} < d \leq 2.000$  mm). In accordance with the guidelines and testing procedures in the Standard for Geotechnical Testing Method (Ministry of Housing and Urban-Rural Development of the People's Republic of China, 2019), a series of fundamental tests was conducted to assess the physical properties of loess samples. The outcomes of these tests are presented in Table 1. Based on the Unified Soil Classification System (USCS) outlined by the American Society for Testing and Materials (ASTM) in 2011 (ASTM, 2011), the loess samples were categorized as low-liquid-limit clay.

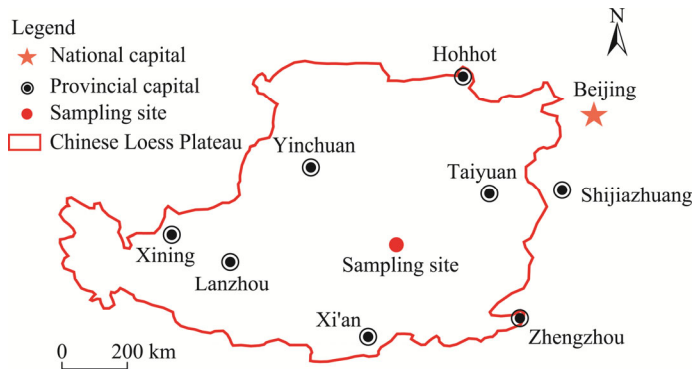


**Fig. 1** Location of the sampling site on the Chinese Loess Plateau

**Table 1** Physical properties of loess samples

Bulk density (g/cm <sup>3</sup> )	Specific gravity	$w$ (%)	$w_p$ (%)	$w_L$ (%)	MDD (g/cm <sup>3</sup> )	OMC (%)	Particle size distribution (%)		
							Clay	Slit	Sand
1.39	2.70	8.92	18.20	28.20	1.50	16.86	11.09	87.39	1.52

Note:  $w$ , natural water content;  $w_p$ , plastic limit;  $w_L$ , liquid limit; MDD, maximum dry density; OMC, optimal moisture content.

### 2.1.2 Polymer SH

The polymer SH, which is an organic curing material, was developed by Lanzhou University. It consists primarily of a hydrophobic macromolecular chain connected by C–C bonds with hydroxyl (–OH) and carboxyl (–COOH) hydrophilic groups interspersed in the chain. This polymer has a density of 1.09 g/cm<sup>3</sup> and an approximate molecular weight of 20,000.

As previously reported by Wang (2016), the optimal conditions to treat loess with polymer SH were determined through a comprehensive analysis of the impact of polymer SH concentration and curing time on various physical and mechanical properties of loess. These properties included enhancements in the compressive strength, shear strength, compressibility, and permeability of polymer SH-treated loess. Using this decision-making process, previous mechanical tests on the treated loess revealed that a curing period of 28 d and an application rate of 3.00% polymer SH constituted the optimal conditions for the polymer SH treatment of loess. Consequently, this study opted to spray the loess samples with a 3.00% concentration of polymer SH and required it to cure for 28 d.

### 2.1.3 Ryegrass

Perennial ryegrass (*Lolium perenne* L.) has been extensively used to manage soil and water loss in loess regions. This grass species boasts a high germination rate, rapid growth, and a relatively low seed price, which make it easily accessible (Young et al., 1975). Considering the sowing expertise in the loess sampling site and specific test conditions, the planting densities of ryegrass were established at 20 and 40 g/m<sup>2</sup> for comparative purposes. Since ryegrass takes more than two weeks to establish its root system, a curing period of 28 d was determined for the loess treated with ryegrass. Moreover, a data collection period of 22 d was used to reveal the influence pattern of ryegrass growth duration on the soil water-holding capacity.

In this study, six groups of untreated and treated loess samples were established for the tests to assess their water-holding characteristics and disintegration abilities (Table 2). Each group had three parallel samples; in the analysis of the results, the average value of the measurements from three parallel samples was calculated and adopted as the final result.

## 2.2 Methods

### 2.2.1 Monitoring the volumetric water content and water potential of loess samples

In the experiments conducted to monitor soil volumetric water content and water potential, the

**Table 2** Information about the untreated and treated loess samples

Group	Polymer SH content (%)	Ryegrass planting density (g/m <sup>2</sup> )	Group	Polymer SH content (%)	Ryegrass planting density (g/m <sup>2</sup> )
A	0.00	0	D	3.00	0
B	0.00	20	E	3.00	20
C	0.00	40	F	3.00	40

Note: The loess samples were prepared at the MDD and OMC. The thousand-grain weight of ryegrass was 1.94 g. The ryegrass planting densities of 20 and 40 g/m<sup>2</sup> can be converted to 10,309 and 20,618 grains/m<sup>2</sup>, respectively.

dimensions of each set of parallel loess samples were uniformly 30.0 cm×40.0 cm×20.0 cm. The preparation process comprised several crucial steps. First, thoroughly air-dried and sieved loess was prepared. Second, a polymer SH solution was sprayed onto the loess surface at a concentration of 3.00% to ensure uniform mixing according to the preset maximum dry density (MDD) and optimal moisture content (OMC), at 1.50 g/cm<sup>3</sup> and 16.86%, respectively. Third, the loess samples were shaped to adhere to the specified dimensions of 30.0 cm×40.0 cm×20.0 cm. Fourth, ryegrass seeds were sown onto the surface of loess samples, followed by the application of a 0.5–1.0 cm thick layer of nutrient soil, which was peat soil blended with perlite to promote the ryegrass growth. Fifth, the loess samples were transferred to a plastic greenhouse and cured for 28 d.

A comprehensive setup was devised to monitor the volumetric water content and water potential of loess samples during the curing process. As depicted in Figure 2, since the ryegrass root depth is 4.0–9.0 cm, water content sensors (EC-5, Beijing Haohan Technology Co., Ltd., Beijing, China) with a measurement range of 0.00%–100.00% and water potential sensors (TEROS 21, Shenzhen Jiuzhou Industrial Products Co., Ltd., Shenzhen, China) with a measurement range from −9 to −100,000 kPa were buried 10.0 cm below the top loess surface. These sensors were integrated with a data collector (Em50, Beijing Dorgean Electronic Technology Co., Ltd., Beijing, China) for efficient data retrieval. Furthermore, flora detectors were inserted into the loess to monitor the ryegrass growing environment and ensure optimal conditions for ryegrass growth, including suitable temperature and adequate illumination. Notably, due to the immature root system of ryegrass in the first week after planting, the volumetric water content and water potential of loess samples were not measured. Data collection commenced one week after the ryegrass had been planted.

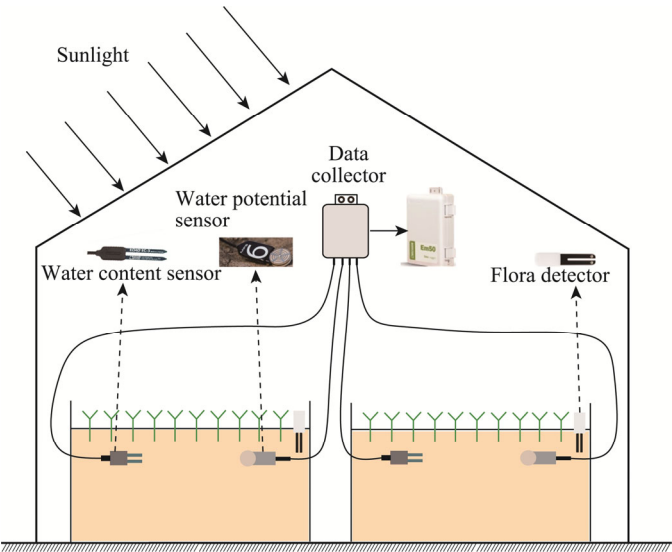


**Fig. 2** Schematic diagram of the soil volumetric water content and soil water potential monitoring devices in this study

The irrigation method in this paper is based on the plant growth status approach. Before initiating the formal experiment, extensive preliminary experiments were conducted to determine the optimal irrigation volume for the trial. Insights from these preliminary studies led to the implementation of a consistent spraying regime of 200 mL of water at noon each day during the initial week after the ryegrass was planted. This approach aims to increase seed germination and ensure adequate soil moisture. After the ryegrass sprouted, the irrigation schedule was adjusted. Factors such as the growth rate of branches and leaves, wilting of tender leaves, and colour changes in stems and leaves were considered and resulted in the decision to water the plants with 200 mL of water once a week. Once the ryegrass had completed its growth cycle, watering was discontinued to mimic an arid environment. This model experiment was conducted from August to December in 2023.

### 2.2.2 Fractal pore theory

The fractal method involves establishing a soil-water characteristic curve parameterized by clearly defined physical meanings (Tyler and Wheatcraft, 1990; Huang and Zhang, 2005). Using fractal theory, fractal dimensions can be straightforwardly derived from the measured soil-water characteristic curve data. The fractal dimension has a direct correlation with the soil pore structure, where a higher fractal dimension corresponds to a lower soil porosity (Tao et al., 2014).

The fractal model, which reflects the soil volumetric water content and soil matrix suction in this study, was introduced and validated by Tao et al. (2014). This expression is as follows:

$$\theta_w = \phi - 1 + (h_{\max} / h)^{3-D}, \quad (1)$$

where  $\theta_w$  is the soil volumetric water content (%);  $\phi$  is the total soil porosity (%);  $h_{\max}$  is the soil matrix suction corresponding to the maximum pore diameter (kPa);  $h$  is the soil matrix suction (kPa); and  $D$  is the fractal dimension.

The total energy of soil can be expressed as (Li et al., 2006):

$$E = m_w g z - \frac{m_w h}{\rho_w}, \quad (2)$$

where  $E$  is the total energy of soil (J);  $m_w$  is the mass of water in the soil body (kg);  $g$  is the gravitational acceleration ( $\text{m/s}^2$ );  $z$  is the relative height (m); and  $\rho_w$  is the water density in the soil body ( $\text{kg/m}^3$ ).

The water potential ( $E_w$ ; kPa), which is the water energy per unit soil volume, can be expressed in conjunction with Equation 2 as:

$$E_w = \rho_w g z - h. \quad (3)$$

Assuming a constant water density of  $1000 \text{ kg/m}^3$ , since the measurements from the apparatuses during the experiment are uniform in height, the relative height can effectively be considered as zero. Consequently, the soil matrix suction is equivalent to the absolute value of the soil water potential. Based on Equation 1, the relationship between soil volumetric water content and soil water potential can be expressed as:

$$\theta_w = \phi - 1 + (E_{w\max} / E_w)^{3-D}, \quad (4)$$

where  $E_{w\max}$  is the soil water potential for the maximum pore diameter (kPa).

The relationships among the total soil porosity, soil dry density, and specific gravity can be expressed as follows:

$$\phi = 1 - \frac{\rho_d}{G_s}, \quad (5)$$

where  $\rho_d$  is the soil dry density ( $\text{kg/m}^3$ ), which was controlled at  $1500 \text{ kg/m}^3$  in this study; and  $G_s$  is the specific gravity, which was set as 2.70 in this study.

We substituted Equation 5 into Equation 4 and took the logarithm on both sides of Equation 4. The correlation between soil volumetric water content and soil water potential can be derived as follows:

$$\ln\left(\theta_w + \frac{\rho_d}{G_s}\right) = (3 - D)[\ln(-E_{w\max}) - \ln(-E_w)] \quad (6)$$

After establishing the characteristic curve defined by the soil volumetric water content and soil water potential (the negative value of soil matrix suction), one can construct a scatter plot using  $-\ln(-E_w)$  as the abscissa and  $\ln(\theta_w + \rho_d/G_s)$  as the ordinate. If the points on this plot exhibit a linear relationship and assuming that the slope of the line is  $k$ , then the fractal dimension (calculated using  $3-k$ ) can be used to demonstrate the fractal nature of the soil pore distribution. Fractal dimension can effectively represent the changes in soil pore structure.

### 2.2.3 Disintegration test

Disintegration test was conducted using a self-designed instrument to assess the disintegration characteristics of loess samples in October 2023. Figure 3 shows that a cylindrical loess sample measuring 61.800 mm×40.000 mm (diameter×height) was submerged in water. A metal plate with a uniformly distributed mesh was used to position the test loess sample. The dimensions of the metal plate and mesh were 10.0 cm×10.0 cm and 10.000 mm×10.000 mm, respectively. A digital dynamometer directly attached to the metal plate was used to document the mass changes of the test loess sample during the disintegration process. These dynamometer readings were automatically transmitted to a computer via a USB cable to quantitatively analyse the mass changes of the test loess sample over time during disintegration. The test was completed when the test loess sample was completely disintegrated or when the testing duration reached 24 h.

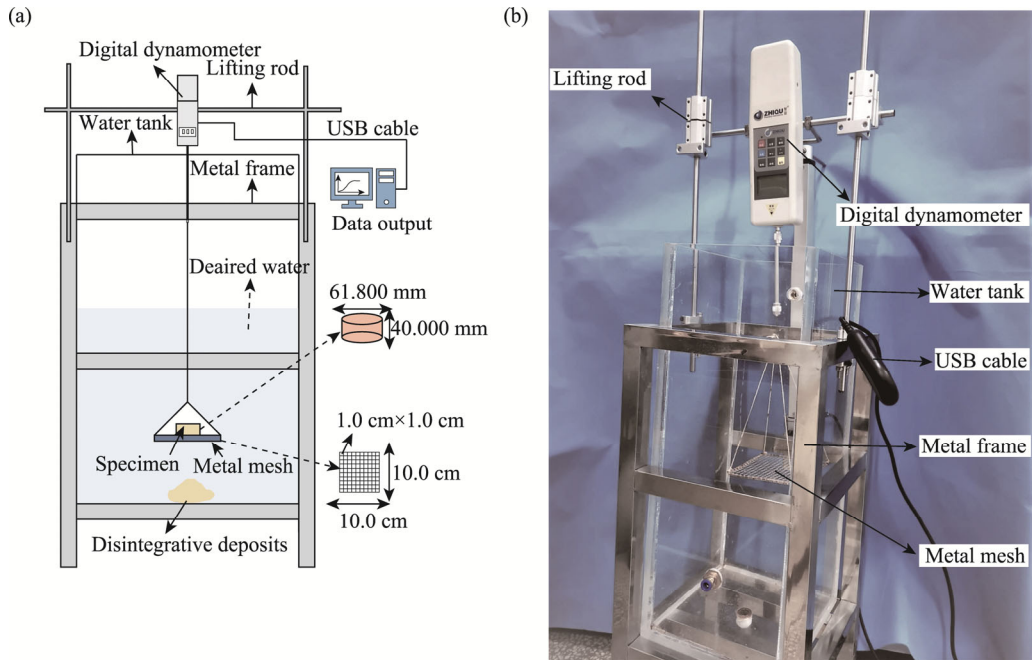


**Fig. 3** Schematic diagram (a) and photograph (b) of the apparatus in the disintegration test

Data obtained from the digital dynamometer were used to compute the disintegration ratio of loess samples, which can be expressed as:

$$A_t = \frac{R_1 - R_t}{R_1 - R_0} \times 100\%, \quad (7)$$

where  $A_t$  is the disintegration ratio of the test loess sample (%);  $R_1$  is the floating weight of an unbroken loess sample determined through parallel tests on wax-sealed samples (N);  $R_t$  is the dynamometer reading at a specific time  $t$  (N); and  $R_0$  is an apparatus constant that reflects the combined weight of the metal wire and metal plate when the test loess sample is absent (N).



### 3 Results

#### 3.1 Variations in the volumetric water content of loess samples under different treatments

Figure 4 shows the fluctuations in the volumetric water content of loess samples across various curing durations. Considering the distinct initial impacts exerted by the preparation of loess samples and ryegrass planting, the initial volumetric water content of loess samples varied across the six tested groups. The volumetric water content consistently decreased across all groups at a gradually decreasing rate over time. Following watering on days 12 and 17, the volumetric water content of loess samples experienced a transient increase in the subsequent 24 h. When watered 200 mL weekly, the surge in the volumetric water content of loess samples was generally more pronounced following the initial watering, due to the initial arid conditions. Overall, during the experimental period, on any given day, the ranking of the volumetric water content of loess samples among the groups was as follows: Group E>Group F>Group D>Group B>Group C>Group A. When the rate of decline in the volumetric water content of loess samples was calculated by comparing the first day and the last day of the experiment, the following descending order of decline rates was observed: Group E (25.27%)<Group F (33.49%)<Group D (36.90%)<Group B (37.63%)<Group C (39.01%)<Group A (42.31%).

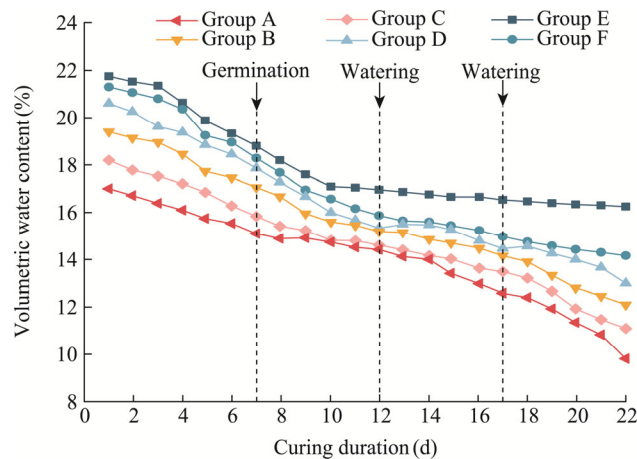


**Fig. 4** Variations in the volumetric water content of loess samples from the six groups (A, B, C, D, E, and F) with varying curing durations

The loess treated with polymer SH (Groups D, E, and F) presented a higher volumetric water content than the loess without polymer SH treatment (Groups A, B, and C) on the same day of the experiment. When the same amount of polymer SH was added, the ryegrass-treated loess had higher volumetric water content than the loess without ryegrass treatment. For example, the volumetric water content of loess samples from both Groups E and F surpassed that of loess samples from Group D, which demonstrated the effectiveness of ryegrass in increasing the volumetric water content of Chinese loess. This increase can be probably attributed to the following reasons: the leaves of ryegrass serve to obstruct a portion of sunlight and diminish the direct solar radiation that reaches the soil surface. Furthermore, the transpiration process of the plants forms a humid air layer, which contributes to the water retention on the soil surface (Grantz, 1990; Lambers et al., 2008).

The improvement in the volumetric water content of Chinese loess caused by ryegrass was closely related to the ryegrass planting density, where Group E (20 g/m<sup>2</sup> ryegrass planting density) had higher volumetric water content than Group F (40 g/m<sup>2</sup> ryegrass planting density). The reasons behind this phenomenon are as follows: when ryegrass is planted at a high density, competition between plants increases, and the plants require more water to meet their growth demands (Zhang et al., 2019). This competition may accelerate the rate of soil moisture



consumption and reduce the water-holding capacity. However, when ryegrass is planted at a relatively lower density, competition for soil water among ryegrass plants is reduced, and each plant can more easily access the required water, which results in relatively stable changes in soil water content.

Group E, which used a combination of polymer SH and ryegrass at a relatively lower planting density, had the highest water-holding capacity. This result reflects the synergistic effects of the combination of polymer SH and ryegrass. As previously mentioned, polymer SH can effectively enhance the water-holding capacity of loess through its intricate spatial network. Additionally, ryegrass can mitigate the impact of direct solar radiation on the soil surface, whereas its transpiration process contributes to the establishment of a humid air layer.

### 3.2 Variation in the water potential of loess samples under different treatments

Figure 5 shows the variations in the water potential among the loess samples with various curing durations. The trend of the water potential over the first 22 d was largely consistent with the changes observed in the first 10 d (Fig. 5a and b). The loess treated with polymer SH (Groups D, E, and F) had higher water potentials than the untreated loess (Groups A, B, and C). In addition, the loess treated with ryegrass (Groups B and C) had higher water potentials than the untreated loess (Group A). This phenomenon was consistent with the observed changes in the volumetric water content (Fig. 4). Specifically, the polymer SH-treated groups presented higher water potentials than the polymer SH-free groups, and the ryegrass-treated groups presented greater water potential than the untreated groups. The water potential, which indicates the energy state of water in soil, increases with increasing water content (Bryan, 2000; Or and Wraith, 2002). Consequently, under identical experimental conditions, soils with higher volumetric water contents tend to have higher water potentials.

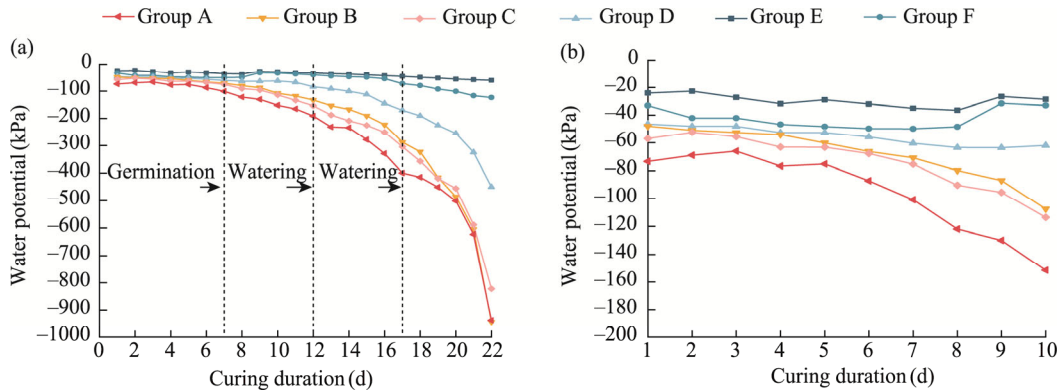


**Fig. 5** Variations in the water potential of loess samples from the six groups (A, B, C, D, E, and F) with varying curing durations. (a), curing durations of 1–22 d; (b), curing durations of 1–10 d.

Group E exhibited the highest water potential among the groups. Through physical-chemical interactions with loess, polymer SH can strengthen the connections among loess grains (Wang et al., 2005). Consequently, the spatial structure of the loess-ryegrass system may be strengthened by polymer SH, which enhances the water-holding capacity of loess. In addition, Group E had higher volumetric water content and water potential than Group F (Figs. 4 and 5), which clearly indicated that in the present study, the feasibility of the combined technique lies in combining polymer SH with a lower ryegrass planting density.

### 3.3 Fractal characteristics of the volumetric water content and water potential of loess samples under different treatments

The volumetric water content and water potential of loess samples under different treatments for curing durations of 8–21 d were taken separately and subjected to linear fitting using Equation 6. The fitting results are presented in Figure 6, and Table 3 also lists the corresponding correlation

coefficient, fractal dimension, and soil water potential for the maximum pore diameter.

The correlation coefficients for all six groups were remarkably high, which effectively demonstrates the applicability of the fractal dimension calculation method in this study. The volumetric water content and water potential of loess samples displayed notable fractal behaviours, which intrinsically reflects the strong fractal properties of the soil mass pore distribution. Table 3 shows the ranking of the calculated fractal dimensions: Group E>Group D>Group F>Group B>Group C>Group A. In addition, the fractal dimension was directly proportional to both volumetric water content and water potential. For example, for curing durations of 8–21 d, Group E had the highest fractal dimension (2.978; Table 3), highest volumetric water content (Fig. 4), and highest water potential (Fig. 5) among all groups. This finding indicated that when exposed to certain relative humidity levels under different conditions of relative humidity, the soil water potential increases and the soil pore volume decreases, which improves the water-holding capacity and increases the fractal dimension. Similarly, as the soil pore volume decreases, the fractal dimension increases and the volumetric water content decreases (Russell, 2014; Liao et al., 2022; Yang et al., 2023).

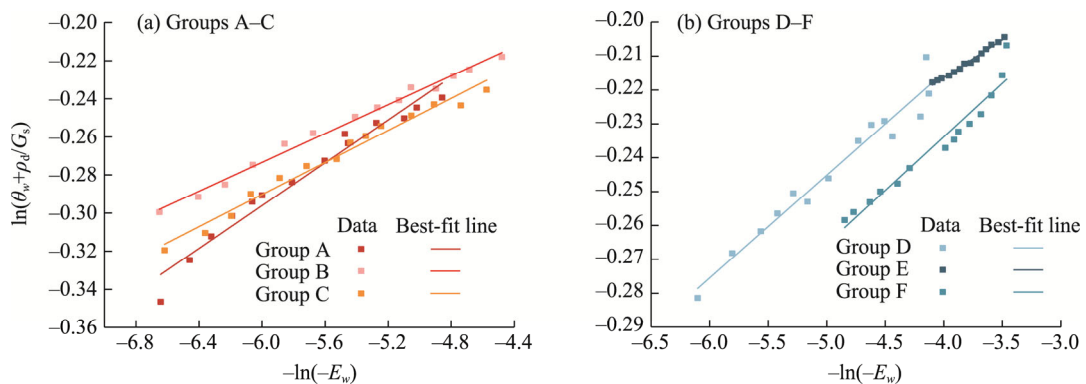


**Fig. 6** Relationships between volumetric water content and water potential of loess samples subjected to different treatments. (a), Groups A–C; (b), Groups D–F.  $\theta_w$ , soil volumetric water content;  $\rho_d$ , soil dry density;  $G_s$ , specific gravity;  $E_w$ , soil water potential.

**Table 3** Parameter calculation of fractal characteristics for loess samples under different treatments

Group	$D$	$r$	$E_{wmax}$ (kPa)	Group	$D$	$r$	$E_{wmax}$ (kPa)
A	2.944	0.96	−1.01	D	2.970	0.96	−0.97
B	2.962	0.99	−0.98	E	2.978	0.99	−0.96
C	2.958	0.98	−0.99	F	2.968	0.95	−0.97

Note:  $D$ , fractal dimension;  $r$ , correlation coefficient;  $E_{wmax}$ , soil water potential for the maximum pore diameter.

## 4 Discussion

The soils on the Chinese Loess Plateau are mainly characterized by severe soil erosion and water scarcity, high evapotranspiration rate, and excessive leaching of scant rainfall, leading to poor water use by plants (Fu et al., 2011; Gao et al., 2014). To address these issues, we proposed a new combined treatment involving polymer SH and ryegrass. Our findings revealed that this treatment substantially enhanced the water-holding capacity of Chinese loess. This improvement aligned with the results reported by several scholars who have also documented the effectiveness of polymer SH in increasing soil water-holding capacity (Cao et al., 2017; Hou et al., 2021; Zhang et al., 2023). We collected experimental data after cultivating ryegrass for 28 d with a data collection period of 22 d. Although a 50-d observation period cannot fully reflect the impact of ryegrass on the physical and mechanical properties as well as the water-holding characteristics of loess, it can

reveal the influence pattern of ryegrass growth process on its water-holding capacity. Nonetheless, long-term monitoring is necessary to accurately reflect the impact of vegetation on soil properties in the future. In our experiments, with a combination of 3.00% polymer SH and 20 g/m<sup>2</sup> ryegrass, Group E exhibited the highest volumetric water content and water potential and a calculated fractal dimension of 2.978, reflecting the fractal characteristics of the soil structure with the lowest soil porosity. For a deeper insight into the implications of these findings for soil structure, an analysis of soil structural stability offers a crucial perspective. The structural stability of loess can be assessed via wet disintegration tests, where the disintegration ratio of loess highly depends on the degree of particle cementation, pore structure, and soil porosity (Xie et al., 2018; Li et al., 2019; Xu et al., 2022). Here, six groups of disintegration tests were conducted on untreated and treated loess samples to investigate their structural stability.

The disintegration test results of various treated loess samples are presented in Figure 7. Figure 7a depicts their disintegration behaviour over time from 0 to 1000 s, and Figure 7b focuses on the first 180 s. From an extended observation period of 1000 s, all loess samples exhibited a notable increase in disintegration ratio from 0 to approximately 500 s and a slight increase from 500 to 1000 s (Fig. 7a). Since the disintegration resistance of a loess sample can be determined from its disintegration ratio, a ranking of the anti-disintegration ability of loess samples can be drawn: Group D>Group E>Group F>Group A>Group B>Group C. This result showed that the single polymer SH treatment (Group D) was the most effective at reducing loess disintegration, since it had a significantly stronger anti-disintegration ability than the single ryegrass treatment, combined polymer SH and ryegrass treatment, and control (without treatment). In addition, the ranking of Group A above Group B showed that ryegrass roots can adversely affect the soil aggregate stability, but this influence could be greatly eliminated by the polymer SH treatment, since Group E ranked above Group A.

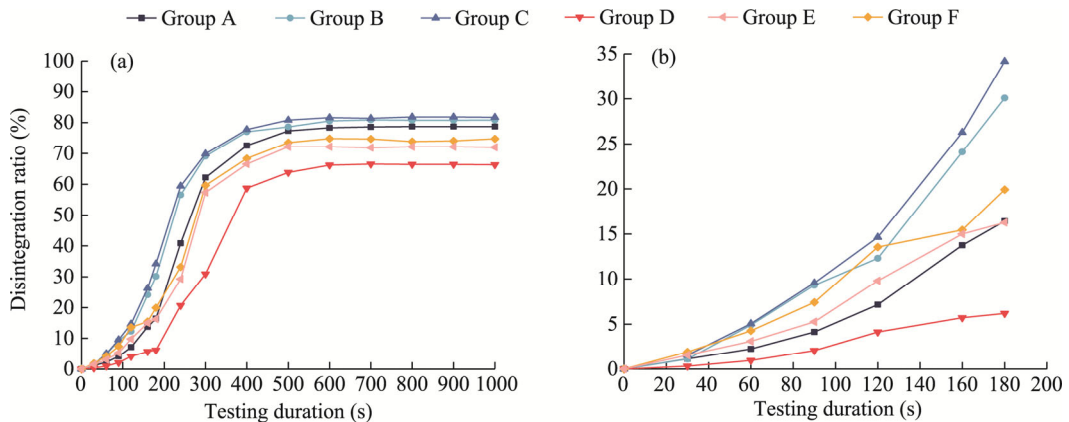


**Fig. 7** Results of the disintegration tests on six groups (A, B, C, D, E, and F) of loess samples. (a), testing durations of 0–1000 s; (b), testing durations of 0–180 s.

The improvement in anti-disintegration ability of loess by polymer SH was proven to be related to the physical and chemical interactions between polymer SH and loess (Wang et al., 2005; Hou et al., 2021). When the physical interactions are considered, polymer SH can fill the pores in the soil, which creates a spatial network structure that envelopes the soil particles and effectively hinders water infiltration into the soil (Hou et al., 2021; Ying et al., 2024). With respect to chemical interactions, ion exchange reactions between polymer SH and loess clay particles can occur, which will change the electrochemical state of the double layer surrounding clay particles and subsequently enhance the attraction among clay particles (Wang, 2016). In addition, a hydrogen bond may form between the carboxyl (–COOH) of polymer SH and the hydroxyl (–OH) groups on the surfaces of silicates (Wang et al., 2005).

Figure 7b shows that the initial disintegration ratios during the first 180 s of the ryegrass-treated loess (Groups B, C, E, and F) were greater than those of the ryegrass-free groups (Groups A and D). The detrimental effect of ryegrass on the soil disintegration performance is intricately linked to the modifications in soil pores caused by the growth of ryegrass roots (Angers and Caron, 1998). Water movement and gaseous diffusion are considerably promoted by the soil macropores created by plant roots penetrating the soil, which improves the connectivity of the pore system and infiltration capacity of the soil (Gyssels et al., 2005; Fischer et al., 2015). Thus, the enhanced infiltration capacity can expedite aggregate breakdown and disintegration and result in a higher disintegration ratio, as found in ryegrass-treated loess.

The disintegration ratios (Fig. 7) and calculated fractal dimensions (Table 3) of loess samples lacked significant relevance. For example, Group E presented the highest fractal dimension, but its anti-disintegration ability was not the highest among the groups and was inferior to that of Group D. This discrepancy is reasonable because ryegrass roots adversely impact the soil aggregate stability and potentially mitigate the positive influence of polymer SH on the disintegration resistance of the combined polymer SH and ryegrass treatment (Ying et al., 2024). Notably, although Group E had lower soil structural stability than Group D, it was more stable than the other four groups, so its structural stability was relatively good.

## 5 Conclusions

This study evaluated an innovative approach of using both polymer SH and ryegrass to enhance the water-holding capacity of Chinese loess. A comparative analysis of untreated and treated loess samples highlighted several key outcomes. First, the combined technique of polymer SH and ryegrass significantly improved the volumetric water content and water potential of loess compared to the effects of either treatment alone. This enhancement can be attributed to the synergistic effects of polymer SH and ryegrass, which effectively promotes the water-holding capacity of loess. Notably, the optimal ryegrass planting density for the maximal improvement of loess was identified as 20 g/m<sup>2</sup>. Second, fractal dimension analysis revealed a direct correlation between loess moisture conditions and pore distribution characteristics. When the loess moisture increased, the water potential and fractal dimension increased, which indicates a stronger water-holding capacity. This observation underscored the importance of fractal dimension as an indicator of soil water-holding capacity. Finally, the combined technique outperformed ryegrass alone in terms of disintegration resistance but it did not outperform polymer SH alone. The reason is likely the increased infiltration capacity facilitated by ryegrass roots, which inadvertently reduced the water stability of loess.

In summary, our study demonstrated the potential of the combined technique of polymer SH and ryegrass in enhancing the water-holding capacity of Chinese loess. However, it is necessary to investigate the changes in the physical properties of loess (such as structure, bulk density, and porosity) under different treatments to provide more direct and solid evidence. Future research should delve deeper into additional parameters such as the residual water content and air entry value to characterize the water-holding capacity of treated loess, and provide a more comprehensive understanding of the effectiveness of the proposed technique and guide future applications.

## Conflict of interest

The authors declare that they have no known competing financial interests or personal relationships that could have appeared to influence the work reported in this paper.

## Acknowledgements

This study was supported by the Natural Science Foundation of Qinghai Province (2024-ZJ-987) and the Natural Science Foundation of Qinghai University (2023-QGY-9).

## Author contributions

Conceptualization: YING Chunye, LI Lanxing; Methodology: YING Chunye, LI Chenglong; Investigation: LI Chenglong, ZHOU Chang; Formal analysis: YING Chunye, LI Chenglong, LI Lanxing, ZHOU Chang; Writing - original draft preparation: YING Chunye; Writing - review and editing: LI Lanxing, ZHOU Chang; Funding acquisition: YING Chunye; Supervision: LI Lanxing, ZHOU Chang. All authors approved the manuscript.

## References

- ASTM (American Society for Testing and Materials). 2011. Standard Practice for Classification of Soils for Engineering Purposes (Unified Soil Classification System) (ASTM D2487–98). [2024-05-10]. <https://www.astm.org>.
- Angers D A, Caron J. 1998. Plant-induced changes in soil structure: processes and feedbacks. *Biogeochemistry*, 42(1): 55–72.
- Bryan R B. 2000. Soil erodibility and processes of water erosion on hillslope. *Geomorphology*, 32(3–4): 385–415.
- Cao Y B, Wang B T, Guo H Y, et al. 2017. The effect of super absorbent polymers on soil and water conservation on the terraces of the loess plateau. *Ecological Engineering*, 102: 270–279.
- Chen J S, Chen Y P, Wang K B, et al. 2024. Impacts of land use, rainfall, and temperature on soil conservation in the Loess Plateau of China. *Catena*, 239: 107883, doi: 10.1016/j.catena.2024.107883.
- Chen W W, Zhang Q Y, Liu H W, et al. 2017. Reinforcing effect of relic soil sites penetrated with high polymer material SH. *Journal of Engineering Geology*, 25(5): 1307–1313. (in Chinese)
- Comegna V, Damiani P, Sommella A. 1998. Use of a fractal model for determining soil water retention curves. *Geoderma*, 85(4): 307–323.
- Dong Y Q, Lei T W, Li S Q, et al. 2015. Effects of rye grass coverage on soil loss from loess slopes. *International Soil and Water Conservation Research*, 3(3): 170–182.
- Fischer C, Tischler J, Roscher C, et al. 2015. Plant species diversity affects infiltration capacity in an experimental grassland through changes in soil properties. *Plant and Soil*, 397(1–2): 1–16.
- Fredlund D G. 2006. Unsaturated soil mechanics in engineering practice. *Journal of Geotechnical and Geoenvironmental engineering*, 132(3): 286–321.
- Fu B J, Liu Y, Lü Y H, et al. 2011. Assessing the soil erosion control service of ecosystems change in the Loess Plateau of China. *Ecological Complexity*, 8(4): 284–293.
- Gao X D, Wu P T, Zhao X N, et al. 2014. Effects of land use on soil moisture variations in a semi-arid catchment: implications for land and agricultural water management. *Land Degradation and Development*, 25(2): 163–172.
- Ghanbarian-Alavijeh B, Liaghat A, Huang G H, et al. 2010. Estimation of the van Genuchten soil water retention properties from soil textural data. *Pedosphere*, 20(4): 456–465.
- Gomiero T. 2016. Soil degradation, land scarcity and food security: Reviewing a complex challenge. *Sustainability*, 8(3): 281, doi: 10.3390/su8030281.
- Grantz D A. 1990. Plant response to atmospheric humidity. *Plant, Cell & Environment*, 13(7): 667–679.
- Gyssels G, Poesen J, Bochet E, et al. 2005. Impact of plant roots on the resistance of soils to erosion by water: A review. *Progress in Physical Geography: Earth and Environment*, 29(2): 189–217.
- Haruna S I, Anderson S H, Udawatta R P, et al. 2020. Improving soil physical properties through the use of cover crops: A review. *Agrosystems, Geosciences & Environment*, 3(1): e20105, doi: 10.1002/agg2.20105.
- Hou Y F, Li P, Wang J D. 2021. Review of chemical stabilizing agents for improving the physical and mechanical properties of loess. *Bulletin of Engineering Geology and the Environment*, 80: 9201–9215.
- Huang G H, Zhang R D. 2005. Evaluation of soil water retention curve with the pore-solid fractal model. *Geoderma*, 127(1–2): 52–61.
- Huang L M, Shao M A. 2019. Advances and perspectives on soil water research in China's Loess Plateau. *Earth-Science Reviews*, 199(2): 102962, doi: 10.1016/j.earscirev.2019.102962.
- Jabro J D, Evans R G, Kim Y, et al. 2009. Estimating in situ soil-water retention and field water capacity in two contrasting soil textures. *Irrigation Science*, 27(3): 223–229.
- Koudahe K, Allen S C, Djaman K. 2022. Critical review of the impact of cover crops on soil properties. *International Soil and Water Conservation Research*, 10(3): 343–354.
- Lal R. 2020. Soil organic matter and water retention. *Agronomy Journal*, 112(5): 3265–3277.

- Lambers H, Chapin F S, Pons T L. 2008. *Plant Physiological Ecology*. New York: Springer Science & Business Media, 187–263.
- Leenaars J G B, Claessens L, Heuvelink G B M, et al. 2018. Mapping rootable depth and root zone plant-available water holding capacity of the soil of sub-Saharan Africa. *Geoderma*, 324: 18–36.
- Li H K, Mei L X, Gao H. 2009. The effect of grass orchard on the microclimate of orchard in dryland of the Loess Plateau. *Acta Prata Sinica*, 17(5): 615–620. (in Chinese)
- Li M, Chai S X, Du H P, et al. 2016. Rain erosion resistance of type soils solidified by SH dust suppressant at construction site. *Chinese Journal of Environmental Engineering*, 10(6): 3105–3110. (in Chinese)
- Li S Q, Zhao S F, Wang X Z. 2006. Matric suction of unsaturated soils in one-dimensional steady flow. *Rock and Soil Mechanics*, 27(S1): 90–94. (in Chinese)
- Li X A, Wang L, Yan Y L, et al. 2019. Experimental study on the disintegration of loess in the Loess Plateau of China. *Bulletin of Engineering Geology and the Environment*, 78(2): 4907–4918.
- Liao H J, Liu S H, He Y Q, et al. 2022. Study on fractal dimension of pore size and water retention characteristics of loess. *Journal of Northwest University (Natural Science Edition)*, 52(3): 416–422. (in Chinese)
- Malik R K, Green T H, Brown G F, et al. 2000. Use of cover crops in short rotation hardwood plantations to control erosion. *Biomass and Bioenergy*, 18(6): 479–487.
- Ministry of Housing and Urban-Rural Development of the People's Republic of China. 2008. Standard for Geotechnical Testing Method (GB/T 50145-2008). [2024-05-15]. <http://www.mohurd.gov.cn>. (in Chinese)
- Ministry of Housing and Urban-Rural Development of the People's Republic of China. 2019. Standard for Geotechnical Testing Method (GB/T50123-2019). [2024-05-15]. <http://www.mohurd.gov.cn>. (in Chinese)
- Or D, Wraith J M. 2002. *Handbook of Soil Sciences: Properties and Processes*. New York: CRC Press, 49–84.
- Pittaki-Chrysodonta Z, Moldrup P, Knadel M, et al. 2018. Predicting the Campbell soil water retention function: Comparing visible-near-infrared spectroscopy with classical pedotransfer function. *Vadose Zone Journal*, 17(1): 1–12.
- Qin M. 2016. Experimental study on the influence of root systems on soil anti-erosion durability during the growth of typical grass vegetation in loess regions Shaanxi. MSc Thesis. Xi'an: Shaanxi Normal University. (in Chinese)
- Qin Y H, Liu F H, Zhou Q. 2008. Influencing factors of compressive strength of solidified inshore saline soil using SH lime-ash. *Journal of Central South University of Technology*, 15(S1): 386–390.
- Qiu D X, Xu R R, Gao P, et al. 2024. Effect of vegetation restoration type and topography on soil water storage and infiltration capacity in the Loess Plateau, China. *Catena*, 241: 108079, doi: 10.1016/j.catena.2024.108079.
- Ramos J C, Bertol I, Barbosa F T, et al. 2014. Influence of the surface conditions and soil cultivation on water erosion in anceptisol. *Revista Brasileira de Ciência do Solo*, 38(5): 1587–1600.
- Russell A R. 2014. How water retention in fractal soils depends on particle and pore sizes, shapes, volumes and surface areas. *Géotechnique*, 64(5): 379–390.
- Shi H, Shao M A. 2000. Soil and water loss from the Loess Plateau in China. *Journal of Arid Environments*, 45(1): 9–20.
- Suzuki S, Noble A D, Ruaysoongnern S, et al. 2007. Improvement in water-holding capacity and structural stability of a sandy soil in Northeast Thailand. *Arid Land Research and Management*, 21(1): 37–49.
- Tao G L, Kong L W, Xiao H L, et al. 2014. Fractal characteristics and fitting analysis of soil-water characteristic curves. *Rock and Soil Mechanics*, 35(9): 2443–2447. (in Chinese)
- Trindade H, Coutinho J, Jarvis S, et al. 2009. Effects of different rates and timing of application of nitrogen as slurry and mineral fertilizer on yield of herbage and nitrate-leaching potential of a maize/Italian ryegrass cropping system in north-west Portugal. *Grass and Forage Science*, 64(1): 2–11.
- Tyler S W, Wheatcraft S W. 1990. Fractal processes in soil water retention. *Water Resources Research*, 26(5): 1047–1054.
- Vanapalli S K, Fredlund D G, Pufahl D E, et al. 1996. Model for the prediction of shear strength with respect to soil suction. *Canadian Geotechnical Journal*, 33(3): 379–392.
- Wang Y M, Yang Z C, Chen W W, et al. 2005. Strength characteristics and mechanism of loess solidified with new polymer material SH. *Chinese Journal of Rock Mechanics and Engineering*, 24(14): 2554–2559. (in Chinese)
- Wang Y M. 2016. Shear strength characteristics of loess stabilized by new polymer materials. *Low Temperature Architecture Technology*, 38(2): 116–118. (in Chinese)
- Wei Y, Wang Y Q, Han J C, et al. 2019. Analysis of water retention characteristics of oil-polluted earthy materials with different

- textures based on van Genuchten model. *Journal of Soils and Sediments*, 19(1): 373–380.
- Williams K, Caldwell M M, Richards J H. 1993. The influence of shade and clouds on soil water potential: The buffered behavior of hydraulic lift. *Plant and Soil*, 157(1): 83–95.
- Xie J J, Su D R. 2020. Water-holding characteristics of litter in meadow steppes with different years of fencing in Inner Mongolia, China. *Water*, 12(9): 2374, doi: 10.3390/w12092374.
- Xie W L, Li P, Zhang M S, et al. 2018. Collapse behavior and microstructural evolution of loess soils from the Loess Plateau of China. *Journal of Mountain Science*, 15(8): 1642–1657.
- Xu P, Lin Q W, Fang L Y. 2022. Study on the mechanical properties of loess improved by lignosulfonate and its mechanism analysis and prospects. *Applied Sciences*, 12(19): 9843, doi: 10.3390/app12199843.
- Xue P, Fu Q, Li T X, et al. 2022. Effects of biochar and straw application on the soil structure and water-holding and gas transport capacities in seasonally frozen soil areas. *Journal of Environmental Management*, 301(4): 113943, doi: 10.1016/j.jenvman.2021.113943.
- Yang C L, Wu J H, Li P Y, et al. 2023. Evaluation of soil-water characteristic curves for different textural soils using fractal analysis. *Water*, 15(4): 772, doi: 10.3390/w15040772.
- Yang T, Xing X G, Gao Y, et al. 2022. An environmentally friendly soil amendment for enhancing soil water availability in drought-prone soils. *Agronomy*, 12(1): 133, doi: 10.3390/agronomy12010133.
- Ying C Y, Li L X, Makeen G M H, et al. 2024. Erosion control of Chinese loess using polymer SH and ryegrass. *Journal of Mountain Science*, 21(6): 2043–2058.
- Young J A, Evans R A, Kay B L. 1975. Germination of Italian ryegrass seeds. *Agronomy Journal*, 67(3): 386–389.
- Yuan B X, Chen W J, Li Z H, et al. 2023. Sustainability of the polymer SH reinforced recycled granite residual soil: properties, physicochemical mechanism, and applications. *Journal of Soils and Sediments*, 23(1): 246–262.
- Zeng L, Huang Y H. 2010. Study on the evolution of river valleys and geological disasters in the Loess Plateau—A case study of Zichang County, Shaanxi Province. *Chinese Journal of Geological Hazard and Control*, 21(3): 67–72. (in Chinese)
- Zhang H L, Wang G H, Du J, et al. 2023. Effects of several polymeric materials on the improvement of the sandy soil under rainfall simulation. *Journal of Environmental Management*, 345: 118847, doi: 10.1016/j.jenvman.2023.118847.
- Zhang Q Y, Chen W W, Yuan P B. 2020. Experimental study on impregnation and consolidation effects of modified polyvinyl alcohol solution for coarse-grained soils: a case study on the Subashi Buddhist Temple Ruins of China. *Bulletin of Engineering Geology and the Environment*, 79(3): 1487–1500.
- Zhang Q Y, Chen W W, Zhang J K. 2021a. Wettability of earthen sites protected by PVA solution with a high degree of alcoholysis. *Catena*, 196: 104929, doi: 10.1016/j.catena.2020.104929.
- Zhang X C, Zhong Y J, Pei X J, et al. 2021b. A cross-linked polymer soil stabilizer for hillslope conservation on the Loess Plateau. *Frontiers in Earth Science*, 9: 771316, doi: 10.3389/feart.2021.771316.
- Zhang Y H, Wang R, Wang S L, et al. 2019. Effect of planting density on deep soil water and maize yield on the Loess Plateau of China. *Agricultural Water Management*, 223(2): 105655, doi: 10.1016/j.agwat.2019.05.039.
- Zhang Y W, Wang K B, Wang J, et al. 2021c. Changes in soil water holding capacity and water availability following vegetation restoration on the Chinese Loess Plateau. *Scientific Reports*, 11(1): 9692, doi: 10.1038/s41598-021-88914-0.
- Zheng W J, Zeng S Q, Bais H, et al. 2018. Plant growth-promoting rhizobacteria (PGPR) reduce evaporation and increase soil water retention. *Water Resources Research*, 54(5): 3673–3687.
- Zhou Z C, Shangguan Z P. 2007. The effects of ryegrass roots and shoots on loess erosion under simulated rainfall. *Catena*, 70(3): 350–355.
- Zhou Z C, Shangguan Z P. 2008. Effect of ryegrasses on soil runoff and sediment control. *Pedosphere*, 18(1): 131–136.